Australian Journal of Earth Sciences (2005) **52**, (353–364)

Hyperspectral imaging spectroscopy of a Mars analogue environment at the North Pole Dome, Pilbara Craton, Western Australia

A. J. BROWN[1]*, M. R. WALTER[1] AND T. J. CUDAHY[1,2]

[1]*Australian Centre for Astrobiology, Macquarie University, NSW 2109, Australia.*
[2]*CSIRO Division of Exploration and Mining, ARRC Centre, 26 Dick Perry Avenue, Technology Park, Bentley, WA 6102, Australia.*

A visible and near infrared (VNIR) to shortwave infrared (SWIR) hyperspectral dataset of the Early Archaean North Pole Dome, Pilbara Craton, Western Australia, has been analysed for indications of hydrothermal alteration. Occurrence maps of hydrothermal alteration minerals were produced. It was found that using a spatial resolution on the ground of approximately 5 m and spectral coverage from 0.4 to 2.5 μm was sufficient to delineate several hydrothermal alteration zones and associated veins, including phyllic, serpentinitic and chloritic alteration. These results suggest this level of spectral and spatial resolution would be ideal for localising shallow epithermal activity, should such activity have existed, on the surface of Mars.

KEY WORDS: Archaean, hydrothermal, hyperspectral, Mars, North Pole Dome, Pilbara Craton.

INTRODUCTION

In October 2002 an airborne visible and near-infrared to shortwave infrared (VNIR–SWIR or 0.4–2.5 μm) hyperspectral reflectance dataset was collected over the North Pole Dome region of the Early Archaean East Pilbara Granite Greenstone Terrane.

The dataset covers over 600 km^2 of the North Pole Dome (Figure 1), including some of the best exposed outcrops of the 3.5 Ga Warrawoona Group (Van Kranendonk 2000). This region has been the subject of extensive palaeobiological study and has been suggested as a habitat for early life on Earth (Groves *et al.* 1981; Schopf 1993; Walter *et al.* 1980). Hydrothermal veins at the North Pole Dome have been proposed as both a habitat of life (Ueno *et al.* 2004; Van Kranendonk & Pirajno 2004) and a preservation mechanism for biosignatures (Dunlop & Buick 1981). The lateral extent and spatial associations of hydrothermal alteration at the North Pole Dome are thus key factors in understanding the Early Archaean biosphere.

Hyperspectral missions to Mars

The European Space Agency Mars Express orbiter has carried the *Observatoire pour la Minéralogie, l'Eau, la Glace et l'Activité* (OMEGA) instrument (Bonello *et al.* 2004) to Mars and has already returned a large amount of data covering the Martian surface (Bibring *et al.* 2004). The *Compact Reconnaissance Infrared Spectrometer for Mars* (CRISM) instrument is scheduled to launch on the Mars Reconnaissance Orbiter in 2005 and return its first data to Earth in 2006. In order to interpret the spectra obtained by these instruments, Earth analogue investigations are useful, as they offer the opportunity to ground-truth mineral identifications and use this ground-truth to refine spectral-based mapping algorithms. This project has been designed to investigate the ability of a hyperspectral survey to detect and map a hydrothermal system in a Mars analogue environment.

GEOLOGICAL SETTING

The North Pole Dome is a structural dome of bedded, dominantly mafic, weakly metamorphosed volcanic rocks (greenstones) and interbedded ultramafic, felsic and cherty horizons of the 3.51–3.43 Ga Warrawoona Group that dip 30–70° away from the central North Pole Monzogranite, a synvolcanic laccolith emplaced in the core of the dome at 3.46 Ga (Thorpe *et al.* 1992; Van Kranendonk 2000). Minor occurrences of felsic volcanic rocks are interbedded with the greenstones, and these are capped by cherts associated with hiatuses in volcanism (Van Kranendonk & Hickman 2000). The stratigraphy of the North Pole Dome is given in Table 1.

Many authors have attempted to determine the depositional setting of the Warrawoona Group. Early researchers suggested a shallow-marine environment (Buick & Barnes 1984), and recent work has suggested a mid-ocean ridge (Kitajima *et al.* 2001) or oceanic plateau

*Corresponding author: abrown@els.mq.edu.au

ISSN 0812-0099 print/ISSN 1440-0952 online © Geological Society of Australia
DOI: 10.1080/08120090500134530

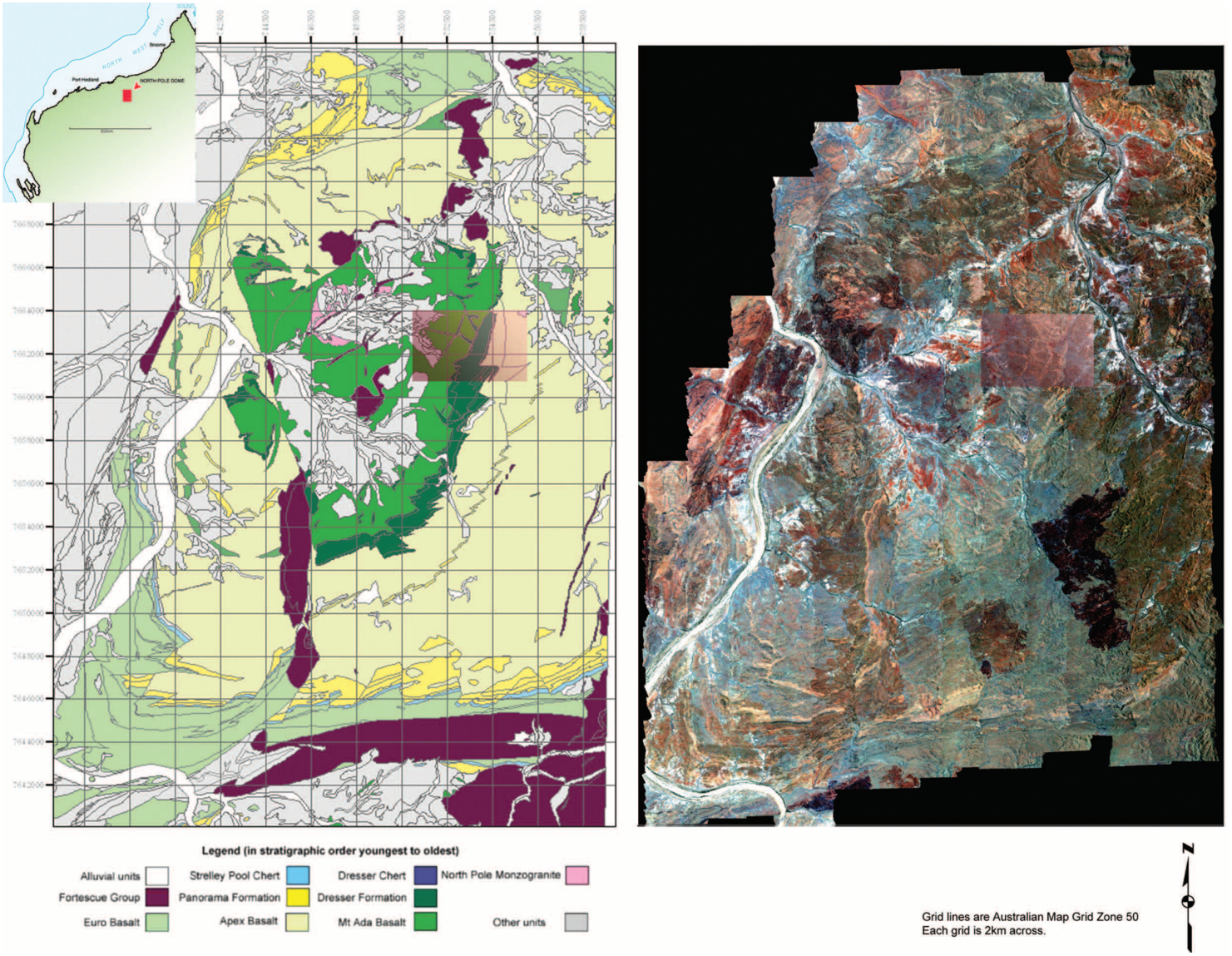

Figure 1 (Left) Simplified geological map of the North Pole Dome (modified after Van Kranendonk 2000). (Right) Visible wavelengths true colour (red: 0.6069 μm, green: 0.5615 μm, blue: 0.4693 μm) image of the hyperspectral dataset. Note 14 swathes have been stitched together and are slightly discontinuous in some regions. Red box indicates the study area (Figure 5).

Table 1 Stratigraphic column of Warrawoona Group units present at the North Pole Dome (Van Kranendonk 2000).

Age (Ga)	Unit	General geology
	Euro Basalt	Ultramafic – mafic volcanic flows, with pillows
3.458	Strelley Pool Chert	Chert – carbonate – clastic sequence
	Panorama Formation	Felsic volcaniclastic suite
	Apex Basalt	Ultramafic – mafic volcanics with some chert horizons
3.470	Duffer Formation	Metamorphosed felsic volcanics
	Dresser Formation	Mafic volcanics
	Mt Ada Basalt	Mafic volcanics, highly metamorphosed
3.515	Coonterunah Group	Basalts with some cherty layers

Dates are derived from U – Pb isotopes from zircons in the units and are accurate to approximately 3 million years (Thorpe *et al*. 1992).

(Van Kranendonk & Pirajno 2004). Stromatolites and putative microfossils have been documented at three different horizons in the North Pole Dome (Dunlop *et al*. 1978; Lowe 1980; Walter *et al*. 1980; Awramik *et al*. 1983; Hofmann *et al*. 1999; Ueno *et al*. 2004).

Hydrothermal activity at the North Pole Dome has been predominantly of a low-temperature, low-pressure (epithermal) type (Barley 1984). Carbonation is broadly restricted to the mafic and ultramafic lavas of the North Pole Dome, whereas pervasive silicification events are most often associated with felsic volcaniclastic horizons and hydrothermal conduits such as those in the Dresser Formation and Strelley Pool Chert (Dunlop & Buick 1981; Lowe 1983).

This study examines a portion of the North Pole Dome dataset covering the upper Dresser Formation and parts of the Apex Basalt (Figure 1). This region was chosen due to the pervasive hydrothermal alteration present at the top of the Dresser Formation.

North Pole Dome as a Mars analogue

Numerous space and planetary science reviews have highlighted the importance of continuing analysis of Earth-based analogues in order to advance the exploration of Mars and the Solar System (McCord 1988; NASA 1995; Space Studies Board 2003; Farr 2004). To this end, many studies of analogue regions in volcanic, arid, biologically extreme environments have been initiated.

The North Pole Dome region is a compelling Mars analogue due to features such as ancient (3.5 billion years old), well-preserved mafic – ultramafic volcanic successions, sparse vegetation, and minimal tectonic metamorphism. In addition, the presence of Earth's earliest biosignatures makes the North Pole Dome an ideal proving ground for strategies to find evidence of past life on Mars (Brown *et al*. 2004).

AIRBORNE IMAGING SPECTROSCOPY

Imaging spectroscopy has been used for more than 20 years to assist economic geologists in remote exploration (Goetz *et al*. 1983). Numerous recent studies have investigated the potential for spectral imaging to map mineral assemblages remotely (Kokaly *et al*. 1998; Stamoulis *et al*. 2001; Bierwirth *et al*. 2002; Kirkland *et al*. 2002; Thomas & Walter 2002; Cudahy 2004; Hellman & Ramsey 2004; Rowan *et al*. 2004). A large collection of papers from the annual Airborne Visual and Infrared Imaging Spectrometer (AVIRIS) workshops is archived at the Jet Propulsion Laboratory AVIRIS website (http://aviris.jpl.nasa.gov/).

Physical effects

When photons impinge upon a surface, they may be transmitted, reflected or absorbed (Wendlandt & Hecht 1966). Reflectance spectroscopy is the measurement (over a range of wavelengths) of the flux of photons reflected from a surface in order to obtain diagnostic information about the material under study. It is a particularly useful technique for spacecraft studying large areas of planetary bodies illuminated by the sun, since there is no requirement to carry onboard a powerful illumination source (McCord 1988).

When panchromatic light interacts with a crystal, it is absorbed in anomalous amounts at particular wavelengths. The regions of anomalous absorption depend on the crystal structure and can be diagnostic for a particular mineral. However, in addition to absorption due to crystal effects, reflectance spectra can be modified by varying grainsize, temperature, pressure and mixing (Singer & Roush 1985; Mustard & Hays 1997; Kirkland *et al*. 2003). These effects can complicate spectral identification algorithms.

Because photons do not penetrate far into solid surfaces, depending on the overall absorption strength of the target, the technique of reflectance spectroscopy is only able to detect minerals within roughly 10 μm of the exposed surface of a rock (Vincent & Hunt 1968). Thick dust, desert varnish, weathering rinds, solids, sand and alluvial coverings can inhibit (or prohibit) the detection of target minerals. The influence of weathering in outback Australia is an obstacle to determination of igneous precursors, as it is in any other geochemical project.

The effects of mixing due to multiple crystal configurations within the instrument's ground instantaneous field of view (GIFOV, i.e. 1 pixel on the ground) has traditionally been analysed in two ways. If the mixing components under consideration are large and well separated (such as two different lava flows), the mixing can be approximated as a linear additive process (linear mixing), where the contribution of each material to the spectrum is proportional to its relative abundance and Beer's law applies (Clark & Roush 1984). However, if the components under consideration are intimately mixed,

such as two components of a bimodal lava flow, or different sized crystals of the same chemical structure (Bishop *et al.* 2003), the mixing can be highly non-linear and the components may not be separable in a quantitative sense. The mixing of materials can make some minor components extremely difficult or impossible to recognise, especially minor carbonate phases (Pontual 1997; Kirkland *et al.* 2001).

Minerals of interest in this study are listed in Table 2, along with their chemical formulae (Deer *et al.* 1992) and typical hydrothermal alteration classes (Thompson & Thompson 1996). These minerals have been chosen as targets since they are detectable in the SWIR (2–2.5 μm) region due to the hydroxyl (OH^-) in their mineral structure. These minerals are also typically found in hydrothermal alteration zones, often in concentric patterns surrounding hot spots (Meyer & Hemley 1967; Lowell & Guilbert 1970).

Detection of minerals using spectroscopy relies on matching the spectra collected to a characteristic feature present in a library spectrum. Several spectral libraries are publicly available and this study primarily used the US Geological Survey Spectral Library version 4. A new version of the library has recently been made available (Clark *et al.* 2003).

Given the amount of information present in the spectra of a mineral, it stands to reason that more information will be available in high resolution spectra (Clark *et al.* 1990). As instrument technology has advanced, the progression from so-called multispectral instruments such as the seven channel LANDSAT series, to the modern day AVIRIS instrument with 256 channels, has meant that laboratory quality spectra are now available to the airborne or orbital imaging spectroscopist. The term hyperspectral is typically used to define an instrument that has in excess of 60 channels. The HyMap instrument, with 126 channels, qualifies as a hyperspectral instrument.

HyMap instrument

Integrated Spectronics (ISPL: www.intspec.com) has developed a series of hyperspectral VNIR–SWIR imaging systems which are commercially flown by HyVista Corporation (www.hyvista.com). This instrument series, called 'HyMap', has been under continuous development since 1998 (Cocks *et al.* 1998). While there are many configuration options for the HyMap instrument, the instrument was outfitted for this project with 126 spectral channels covering the VNIR–SWIR wavelengths between 0.45 and 2.5 μm. The coverage of this part of the spectrum is almost contiguous; however coverage is deliberately sparse in areas of high atmospheric absorption near 1.4 and 1.9 μm. Table 3 details the operating characteristics of the HyMap instrument for this project.

A high signal to noise ratio is vital to provide high-quality spectra that can be confidently interpreted. For imaging spectrometers, the signal to noise ratio is strongly influenced by the number of photons arriving at the instrument over any part of the spectrum (Schott 1996). Diminishing numbers of photons are available at wavelengths higher than 0.5 μm due to the nature of the solar response function. Parts of the spectrum affected by atmospheric absorption will also allow fewer photons to reach the instrument, thus decreasing the signal to noise ratio. A plot of the measured signal to noise ratio for the HyMap instrument is given in Figure 2.

At the HyMap operating height of around 2400 m above ground level, some turbulence can be experienced. HyMap is mounted on a 3-axis gyro-stabilised platform with an inertial navigation unit and GPS synchronized for recording actual location in time and space as the instrument is operating. This positional data is provided by HyVista to the end user.

Table 2 Standard formulae of hydroxyl-bearing alteration minerals.

Mineral	Standard formula	Typical alteration class
Phyllosilicates		
Chlorite	$(Mg,Al,Fe)_{12}[(Si,Al)_8O_{20}](OH)_{16}$	Propylitic
Muscovite	$K_2Al_4[Si_6Al_2O_{20}](OH)_4$	Phyllic/sericitic
Kaolinite	$Al_4[Si_4O_{10}](OH)_8$	Argillic
Serpentine	$Mg_3[Si_2O_5](OH)_4$	Serpentinitic
Amphiboles		
Fe-Hornblende	$Ca_2(Mg,Fe)_4Al[Si_7AlO_{22}](OH)_2$	Propylitic/calcic

Formulae from Deer *et al.* (1992); alteration classes from Thompson *et al.* (1996).

METHODOLOGY

HyVista delivers HyMap data as 'radiance at sensor'; therefore the North Pole Dome dataset was first treated in order to retrieve the surface reflectance. The effect of absorption by the atmosphere was removed using the ATREM radiative transfer code (Gao *et al.* 1993). Differences in cross-track illumination caused by the variation in solar angle were removed using a third-order polynomial correction provided by the Cross Track Illumination feature in the computer program ENvironment for Visualising Images (ENVI) (www.rsi.com). In order to enhance absorption features within the spectra, the dataset was treated with the continuum-removal process provided with ENVI (Clark *et al.* 1987). This process removes the spectral back-

Table 3 Operating characteristics of the HyMap VNIR–SWIR spectrometer as configured for this project.

Spectral coverage	0.45 – 2.5 μm (VNIR–SWIR)
No. of channels	126
Operating height	around 2400 m AGL
Instantaneous field of view (IFOV)	2.5 mrad along track, 2.0 mrad across track
Field of view (FOV)	61.3° (512 pixels)
Swathe width	2.3 km
Average ground IFOV (pixel width)	5 m

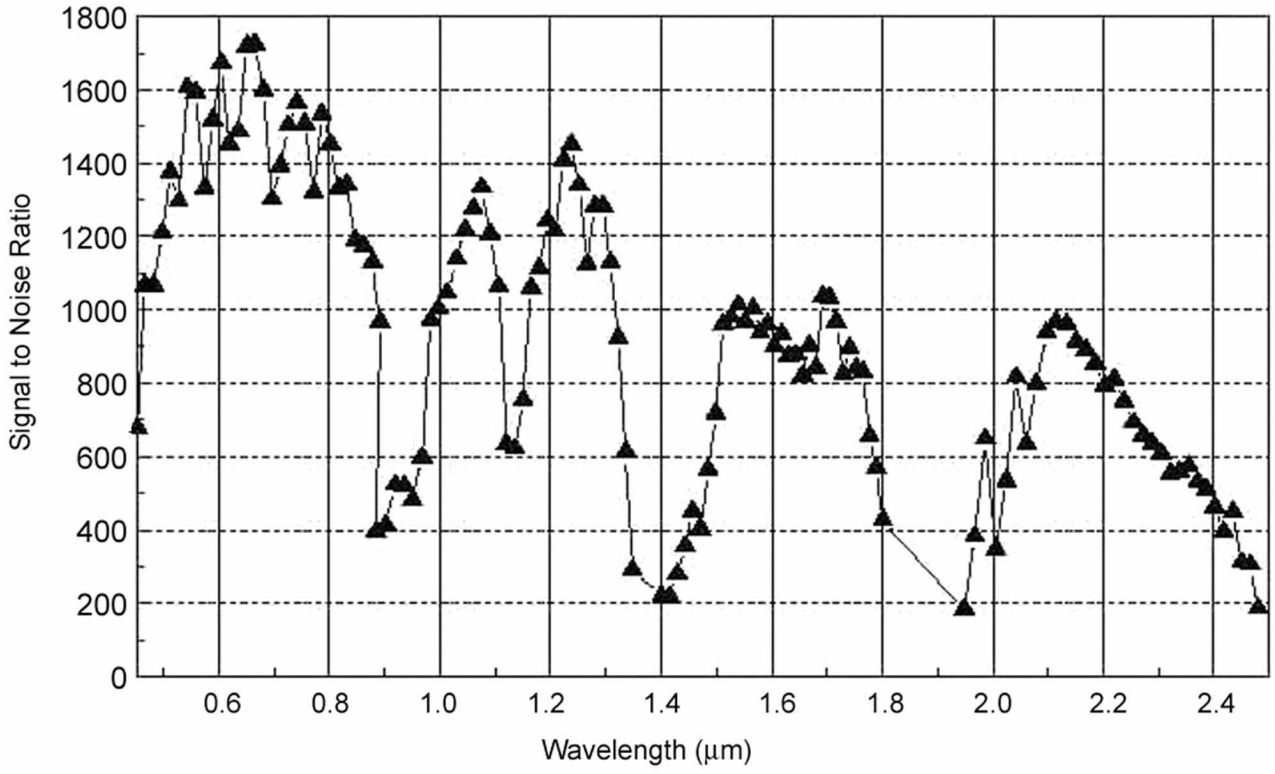

Figure 2 Signal to noise ratio of the HyMap instrument (from Cocks *et al.* 1998).

ground due to electromagnetic scattering and other effects, thus enhancing the depth of absorption bands.

Georectification, the process of relating each pixel in the dataset to its true location on the ground (e.g. correcting for the movement of the aircraft), was carried out using ENVI with flight data files supplied by HyVista. Georectification is carried out as the final step of the analysis since the pixels of the final resultant image are interpolated information rather than real data. After georectification, the multiple flight lines were stitched together as a mosaic using ENVI.

In this project we concentrate on the SWIR region of the spectrum, since this contains distinctive absorption bands directly applicable to hydrothermal minerals. Five library SWIR continuum-removed spectra are illustrated in Figure 3. Unique spectral features have been highlighted. These features were used to generate mineral occurrence maps. An automatic search for these features was carried out in each pixel of the hyperspectral dataset, using a similarity algorithm called Spectral Feature Fitting (Clark *et al.* 1990). This algorithm was chosen because it was found to give best results of all the spectral mapping techniques provided with ENVI (e.g. Spectral Angle Mapper, Binary Encoding, etc.). This judgement was based on each algorithm's ability to produce coherent spatial mineral detections and discriminate against outliers (that create a speckled or noisy appearance in the resultant occurrence map).

In addition to spectral mineral mapping, techniques such as examinations of false-colour images can help to highlight regions of differing mineralogy. In this project, this has been achieved by examining regions in the 2.3 and 2.2 μm regions, and assigning the RGB colour planes to particular HyMap channels in this region. This has the effect of highlighting subtle differences in the absorption bands associated with Mg-OH (2.3 μm) and Al-OH (2.2 μm) vibrations (Hunt 1979).

In order to ground-truth the mineral maps, two field seasons have been carried out and representative samples collected. Primary methods of analysis included transmitted and reflected light analysis of petrographic thin-sections and electron microprobe analysis of polished thin-sections.

RESULTS

The dataset at the North Pole Dome consists of 14 flight lines that are 2.3 km wide on average and from 6 to 22 km long. It was collected on 22 October 2002 from 1030 to 1230 Australian Western Standard Time. The collection date was chosen to minimise green vegetation and thus was at the end of the tropical dry season. The swathes were flown in east to west order, odd swathes flying south, even swathes in a north direction. The average altitude of the aircraft was 2460 m above sea-level and the average elevation of the terrain was 65 m. Representation of the coverage is given in Figure 1. A subset of this area, indicated in Figure 1, has been investigated and is reported on here.

Mineral maps

Figure 4 displays the mineral maps that have been derived for each target mineral. Previous field mapping using airborne photographs has facilitated only the

identification of linear features, each thought to be chert veins or faults (Van Kranendonk 2000). This study has shown that in addition to the chert veins, there are two other vein types, one bearing muscovite and the other rich in hornblende. In addition, the presence of a 5–10 m-thick serpentinised unit above the cherts of the Dresser Formation was previously unrecognised: the unit had been mapped as a carbonated basalt (Van Kranendonk 2000).

The muscovite veins consist of a quartz porphyry where the groundmass has now been completely sericitised. Field checking revealed that most of the veins are of varying width, usually 5–20 m across, although their apparent size in the airborne dataset is greatly exaggerated by the position of the veins atop minor topographic protuberances, resulting in the development of scree slopes rich in muscovite splaying out to each side.

As can be seen from Figure 3, some of the minerals have overlapping identifying features, and this makes them hard to discriminate, especially in the presence of noise. Kaolinite and muscovite are hard to discriminate from each other, and if kaolinite is present it is not possible to say definitively whether muscovite is present. We have adopted a position that if there is a kaolinite feature near 2.16μ, then we cannot say anything about the presence of muscovite; therefore it does not appear in the muscovite map. Talc, chlorite and hornblende are also difficult to discriminate due to overlapping features.

False-colour images

The Mg-OH map (Figure 5a) shows chlorite rich zones in blue. A blue band (1) running north–south at the interface between the Dresser Formation and Apex Basalt is accompanied by several alternating blue and green bands (2). These are interpreted to represent separate volcanic flows. The presence of pillows in the Apex Basalt suggests the bands represent submarine lava flows with slightly differing amounts of iron and magnesium, possibly representing geochemically different flows or different amounts of sea-floor alteration (Terabayashi *et al.* 2003). Pervasive argillic alteration at the Dresser Formation appears in white (4). An outstanding problem at the moment is why some chlorite-rich regions at the top of the Dresser Formation (5) escaped this argillic alteration.

The Al-OH map (Figure 5b) shows minor variations in kaolinite and muscovite mineralogy. Intense muscovite alteration is restricted to the quartz porphyry veins

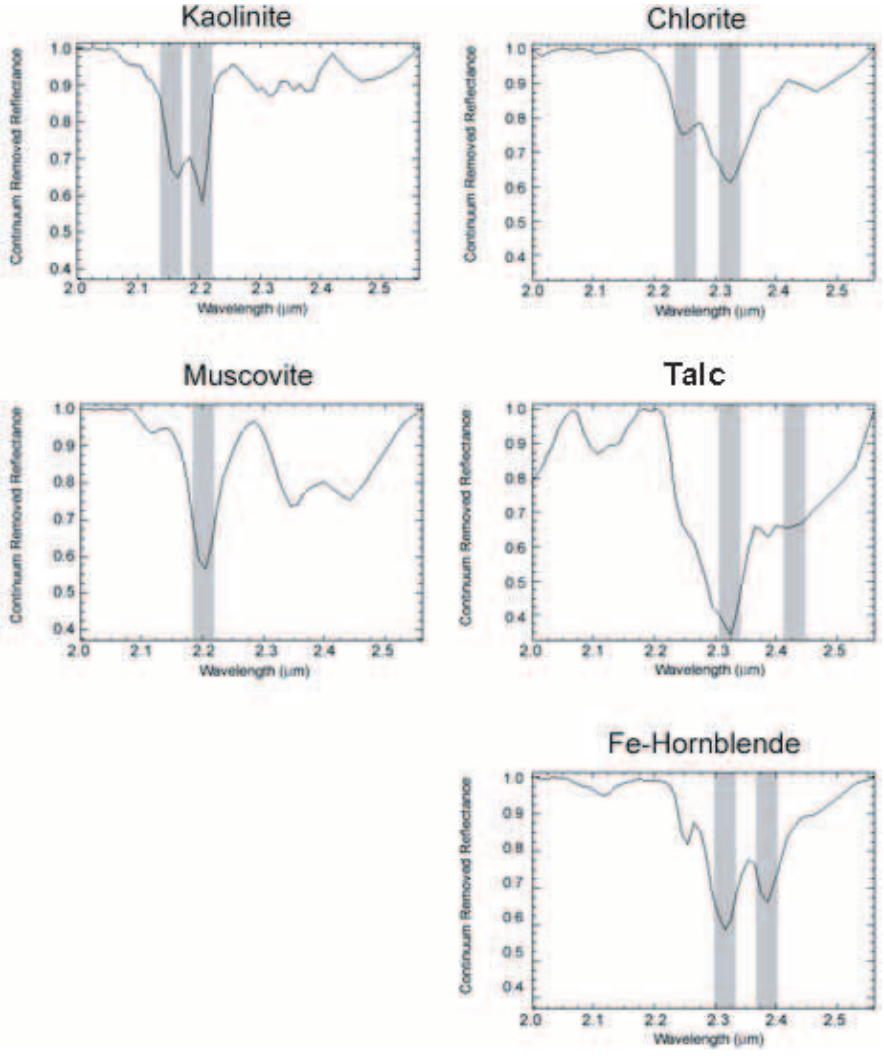

Figure 3 Example SWIR spectra of minerals identified in this study, highlighting unique spectral bands used to identify them. Spectra are taken from the USGS Spectral Library (Clark *et al.* 2003).

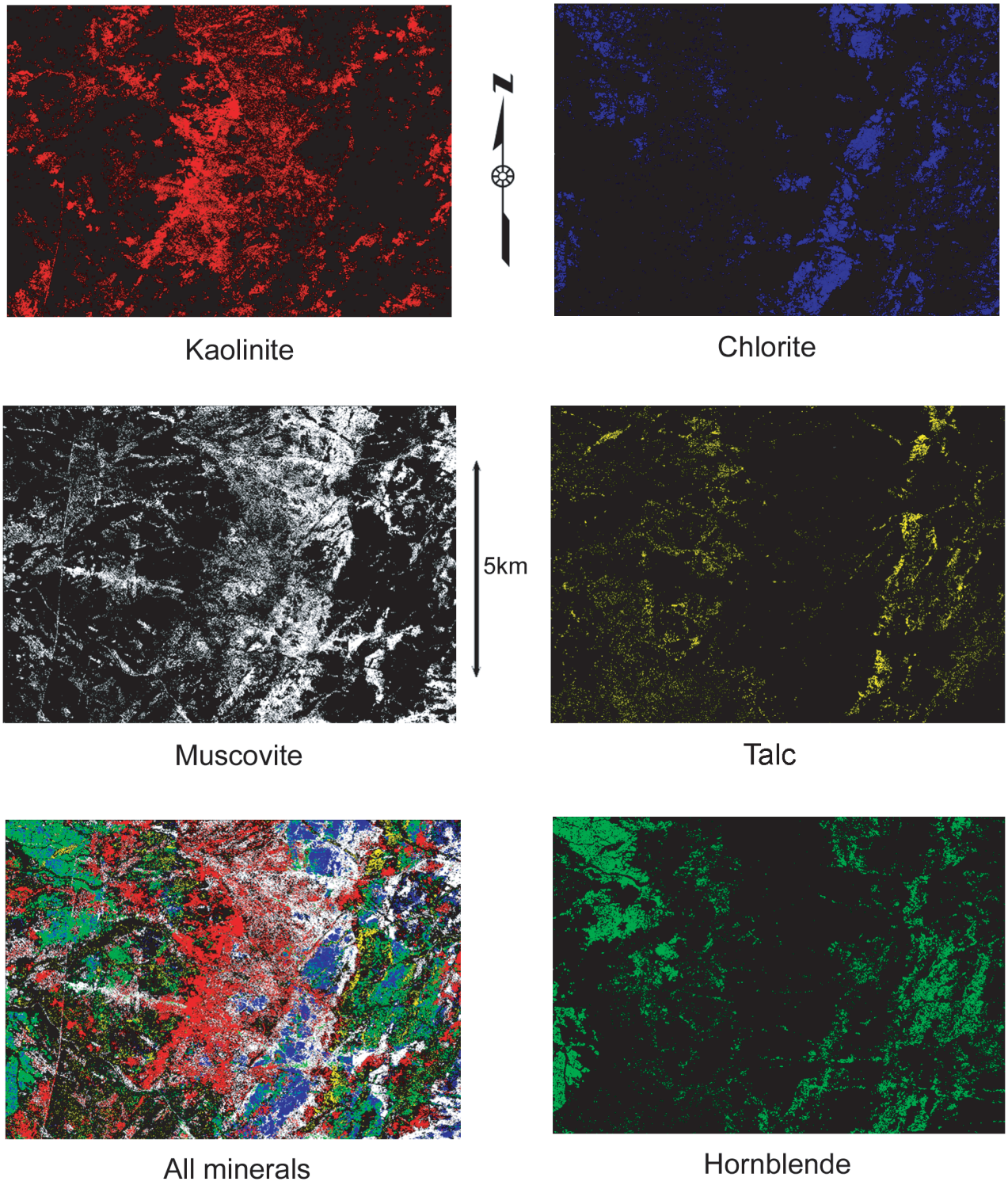

Figure 4 Mineral maps of the study region, showing distributions of the indicated minerals. See Figure 1 for coverage. The image labelled All minerals is a complete hydrothermal zone map, formed by combining the five other maps. Some points are obscured: hornblende (green) was laid down first, then serpentine, then chlorite, then kaolinite, then sericite. This can be viewed as an alteration-class map: white, phyllic zone; red, argillic; blue, propylitic; green, calcic; yellow, serpentinitic.

and associated scree zones (1). Some muscovite seems present in the chert at the top of the Dresser Formation. The grey colour over the basalts of the Dresser Formation indicates a weak but pervasive phyllic–argillic alteration that is restricted to the Dresser Formation (2). This is interpreted to be associated with the presence of the black chert veins which are ubiquitous throughout the unit. Hydrothermal activity associated with these veins, which do not penetrate the overlying Apex Basalt, is likely to have produced a weak sericitisation through-

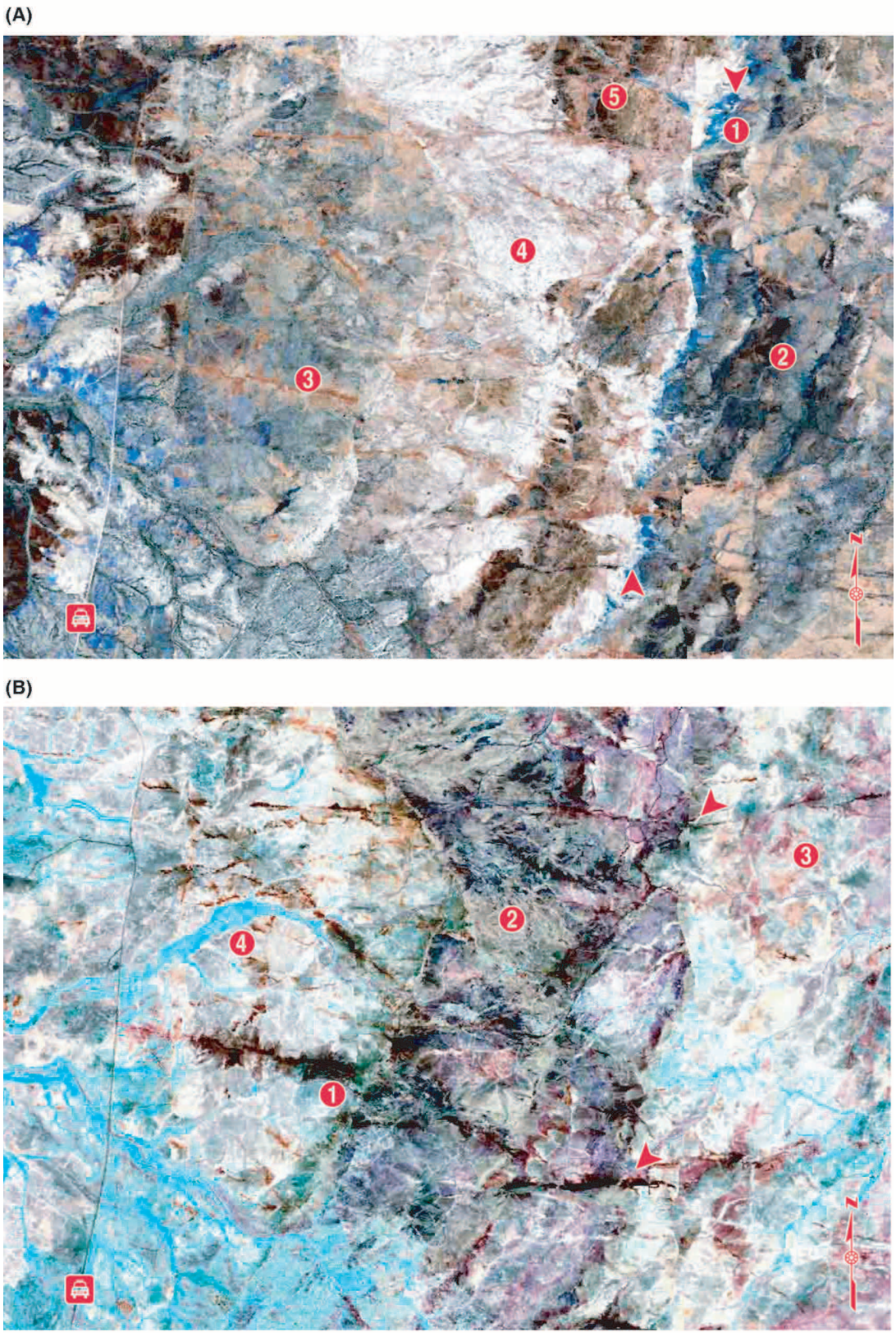

Figure 5 (a) False-colour continuum-removed image showing variations in Mg-OH (chloritisation) mineralogy in study area. Red is assigned to the HyMap channel at 2.3186 μm, green to 2.3348 μm and blue to 2.3515 μm. A thin komatiite layer is in blue, overlying the thin chert layer (in white) at the top of the Dresser Formation (e.g. at point 1). The interface between the Dresser Formation and overlying Apex Basalt runs between the two red arrows. Overlying chlorites in brown and khaki (e.g. at point 2). Muscovite-bearing veins are in light-brown (e.g. at point 3). Pervasively altered basalts of the Dresser Formation are in white (as at point 4). There are unaltered Dresser Formation basalts (coloured brown) beneath (*continued over*)

(*continued from previous*) the white chert layer but above the pervasively altered region (e.g. at point 5). The North Pole Road runs north–south on the left of the image. The image is 5 km wide. See Figure 1 for context. (b) False-colour continuum-removed image showing variations in Al-OH (muscovite/kaolinite) alteration. Region covered is identical to (a), although red is assigned to the HyMap channel at 2.1813 μm, green to 2.1983 μm and blue to 2.2171 μm. Black indicates intense sericitisation along veins (e.g. at point 1), lighter colours indicate little to no white mica present. Grey areas highlight pervasive alteration of the Dresser Formation basalts (e.g. at point 2). Lighter regions with no sericite alteration constitute the Apex Basalt on the right of image (e.g. at point 3). Note that at least two muscovite-bearing veins penetrate the interface between the Dresser and Apex Formations (at arrows). Alluvial fans are highlighted in aqua, e.g. at point 4. The North Pole Road runs north–south on the left of the image. The image is 5 km wide. See Figure 1 for location.

out the Dresser Formation, which is absent from the Apex Basalt above and the Mt Ada Basalt beneath.

Ground-truthing and geochemical analysis

Table 4 gives a summary of mineral phases detected from field samples. Samples were collected from spectrally distinctive units, using the hyperspectral dataset as a guide. Hydroxyl-bearing mineral phases such as chlorite, hornblende, muscovite, kaolinite and talc are all detectable and verified from ground samples.

Ground-truthing of the talc horizon at the interface of the Dresser Formation and Apex Basalt revealed an ultramafic peridotitic komatiite unit, with olivine replaced by serpentine (Brown *et al.* 2004).

Minor problems did occur in some instances, particularly in the west (left) of Figure 4, talc was mapped in some locations but on ground inspection, only carbonatised basalts were found—carbonate does have an absorption at 2.3 μm which overlaps with talc. Work is continuing to address these problems and refine the algorithms used.

Quartz is present in the muscovite-bearing veins, although it is not detectable as a mineral phase in the VNIR hyperspectral dataset, therefore it has not been discussed. Feldspars and pyroxenes are generally not discrimated in the SWIR region. The only sulfate mineral in large quantities in this study, barite, does not have a unique spectral feature in the SWIR. Chert is present in veins in the Dresser Formation, although it is relatively featureless in the VNIR–SWIR. Future versions of HyMap with coverage in the thermal infrared (8–12 μm) may be more successful in mapping these minerals.

Table 4 Mineral phases detected within spectrally distinctive units.

Unit	Field description	Inferred mineralogy from HyMap dataset	Detected mineralogy from hand sample	Analytical methods used
Apex Basalt	Chloritised basalt (with pillows)	Chlorite	Chlorite, epidote, feldspar (albite), pyroxene (diopside)	PTS, EMP
Apex komatiite layer	Ultramafic peridotitic komatiite	Serpentine	Serpentine (antigorite), chlorite, calcite, magnetite	PTS, EMP
Amphibole-bearing veins	Gabbro dyke	Hornblende/chlorite	Hornblende (Fe-rich), chlorite, epidote, calcite	PTS, EMP
Porphyritic veins	Quartz porphyry	Muscovite	Quartz, fine-grained muscovite, minor iron oxides	PTS, EMP
Dresser Formation basalt	Chlorite + sericite altered basalt	Muscovite/kaolinite	Quartz, fine-grained muscovite, kaolinite, chlorite, calcite	PTS, EMP

Units are identified on Figure 1a. PTS, petrographic thin-section; EMP, electron microprobe.

Table 5 Comparison of HyMap (as configured for this project), and the Martian orbiting hyperspectral instruments OMEGA and CRISM.

	Instrument and mode			
	HyMap for Pilbara study	OMEGA	CRISM Hyperspectral	CRISM Multispectral
Approximate pixel size	5 m	300 m – 4.8 km	18–36 m	100–200 m
Spectral coverage	447–2477 nm	350–5090 nm	400–4050 nm	400–4050 nm
Channels	126	484	570	59
Spatial coverage	~28x20 km	~90% of Mars	~11x20 km*	~90% of Mars

* The CRISM Hyperspectral mode is planned to be used at approximately 3000 locations on the Martian surface.

DISCUSSION

High-magnesian lava flows (komatiites), such as those detected in this study at the base of the Apex Basalt, have been suggested to be common on Mars (Baird & Clark 1984). Komatiite shield volcanoes have been proposed as a possible habitat of early life in the Archaean (Nisbet & Sleep 2001). Remote mapping of talc-bearing horizons on Earth and Mars, such as demonstrated here using a VNIR–SWIR hyperspectral sensor, may help to shed new light on likely locations for the origin of life on both planets.

Several studies have suggested the possible emergence or preservation of Martian life at sites of hydrothermal activity (Walter & Des Marais 1993; Shock 1997; Varnes *et al.* 2003). Not all hydrothermal systems marked by alteration should be considered ideal for life. For example, areas of potassic alteration in veins associated with porphyry copper deposits are projected to have formed at 600°C (Sillitoe 1993). This is far in excess of the highest temperatures at which organisms are currently known to grow (Kashefi & Lovley 2003). Epithermal alteration events over deep-seated plutons or on the flanks or distal regions of high-temperature hydrothermal sites, such as those that have been imaged at the North Pole Dome, should be far more suitable for nurturing biological activity similar to life as we know it on Earth (Nealson 1997).

In searching for biosignatures in a hydrothermally altered terrain, regions of chief interest include contacts between varying alteration mineralogies, such as veins or lineaments of a specific alteration type that are discordant with the present terrain. Possible targets for hydrothermal activity on the surface of Mars include crater rims (Brakenridge *et al.* 1985; Cockell & Barlow 2002), volcanic edifices (Farmer 1996), gullies created by hydrothermal activity (Gulick 1998; Harrison & Grimm 2002) and possible shallow intrusions of granitic composition exposed by cratering (Bandfield *et al.* 2004). A shallow granitic intrusion may provide the best chance of finding epithermal alteration similar to that at the North Pole Dome. Scree slopes from elevated areas may enhance the detectability of such deposits, as demonstrated at the North Pole Dome.

The detection techniques used in this project can be applied directly to OMEGA and CRISM data. A comparison of the capabilities of OMEGA, CRISM, and HyMap (as configured for this project) is given in Table 5. HyMap does not cover the 2.5–5.0 μm mid-infrared regions of the spectra to be used by OMEGA and CRISM due to strong absorptions in the Earth's atmosphere in this region. Carbonates and sulfates have unique absorption bands in the 2.5–5.0 μm region, and another strong hydroxyl band occurs at 2.7 μm (Brown 2005). Mineral maps of hydrothermal zones on Mars from OMEGA and CRISM data, analogous to those generated by this study, will be used to determine the distribution of hydrothermal activity on Mars, past and present. Such maps will naturally be of great use in planning landing locations for the upcoming NASA Mars Science Laboratory and the European Space Agency Aurora project ExoMars rover (Vago *et al.* 2003).

CONCLUSION

The results of the hyperspectral mapping of hydrothermal alteration at the North Pole Dome presented herein indicate that hyperspectral imaging is able to provide a synoptic and cohesive assessment of alteration mineralogy over a large area in a relatively short amount of time. Maps such as those in Figures 4 and 5 can be used to direct ground-based studies to identified hot-spots such as contacts between differing alteration types, cross-cutting alteration veins and concentrations of intense alteration.

The results of this study have revealed new details on hydrothermal alteration within the Dresser Formation of the North Pole Dome, and provided a means to separate phyllic, argillic, calcic and propylitic alteration zones. Late stage muscovite- and hornblende-bearing veins have been identified. In addition, the presence of a thin komatiite layer has been discerned at the base of the Apex Basalt.

This study has demonstrated that: (i) in order to detect muscovite-bearing alteration veins and hornblende-bearing gabbro dykes at the scale of those seen in the North Pole Dome, a spatial resolution approaching 5 m is sufficient to discriminate propylitic, phyllic, argillic, calcic and serpentinitic alteration zoning within and surrounding the veins; and (ii) in future VNIR–SWIR hyperspectral surveys of the Martian surface, minerals such as muscovite, chlorite, talc, kaolinite and hornblende provide readily discernable mineral markers (should they be exposed) for mapping hydrothermal alteration zones.

ACKNOWLEDGEMENTS

This research would not have been possible without the generous assistance of the Geological Survey of Western Australia. Assistance in the field and reviews contributed by Martin Van Kranendonk and Michael Storrie-Lombardi were very valuable. The CSIRO Division of Exploration and Mining is thanked for the loan of their PIMA II field spectrometer. Jonathon Huntington and Peter Mason at CSIRO are thanked for their assistance with processing and interpretation of spectra. Terry and Peter Cocks at Integrated Spectronics are thanked for their unwavering support and assistance with field equipment. Thanks to Jeff Byrnes and Guillaume Bonello for thoughtful editing which greatly improved this paper.

REFERENCES

Awramik S. M., Schopf J. W. & Walter M. R. 1983. Filamentous fossil bacteria from the Archaean of Western Australia. *Precambrian Research* **20**, 357–374.

Baird A. K. & Clark B. C. 1984. Did komatiite lavas erode channels on Mars? *Nature* **311**, 18.

Bandfield J. L., Christensen P. R., Hamilton V. E. & McSween H. Y. 2004. Identification of a quartz and Na-feldspar surface mineralogy in Syrtis Major. *Lunar and Planetary Science Conference XXXV*, Abstract 1449.

Barley M. E. 1984. Volcanism and hydrothermal alteration, Warrawoona Group, East Pilbara. *In*: Muhling J. R., Groves D. I. & Blake T. S. eds. *Archaean and Proterozoic Basins of the Pilbara, Western Australia – Evolution and Mineralization Potential*, pp. 23–26. University of Western Australia, Geology Department and University Extension Publication **9**.

Bibring J-P., Langevin Y., Poulet F., Gendrin A., Gondet B., Berthe M., Soufflot A., Drossart P., Combes M., Bellucci G., Moroz V., Mangold N. & Schmitt B. 2004. Perennial water ice identified in the south polar cap of Mars. *Nature* **428**, 627–630.

Bierwirth P., Huston D. & Blewett R. 2002. Hyperspectral mapping of mineral assemblages associated with gold mineralization in the Central Pilbara, Western Australia. *Economic Geology* **97**, 819–826.

Bishop J. L., Drief A. & Dyar M. D. 2003. Physical alteration of Martian dust grains, its influence on detection of clays and identification of aqueous processes on Mars. *6th International Conference on Mars, Pasadena, CA*, 3008. Lunar and Planetary Institute, Houston.

Bonello G., Bibring J. P., Poulet F., Gendrin A., Gondet B., Langevin Y. & Fonti S. 2004. Visible and infrared spectroscopy of minerals and mixtures with the OMEGA/MARS-EXPRESS instrument. *Planetary and Space Science* **52**, 133–140.

Brakenridge G. R., Newsom H. E. & Baker V. R. 1985. Ancient hot springs on Mars: origins and paleoenvironmental significance of small Martian valleys. *Geology* **13**, 859–862.

Brown A. J. 2005. Hydrothermal Mars 'through the CRISM': which hydroxyl band and why. *Lunar and Planetary Science Conference XXXVI*, Abstract 1091.

Brown A. J., Walter M. R. & Cudahy T. J. 2004. Hyperspectral and field mapping of an Archaean komatiite unit in the Pilbara Craton, Western Australia: applications for CRISM mission. *Lunar and Planetary Science Conference XXXV*, Abstract 1420.

Brown A. J., Walter M. R. & Cudahy T. J. 2004. Short wave infrared reflectance Investigation of sites of palaeobiological interest: applications for Mars exploration. *Astrobiology* **4**, 359–376.

Buick R. & Barnes K. R. 1984. Cherts in the Warrawoona Group: early Archaean silicified sediments deposited in shallow water environments. *In*: Muhling J. R., Groves D. I. & Blake T. S. eds. *Archaean and Proterozoic Basins of the Pilbara, Western Australia – Evolution and Mineralization Potential*, pp. 37–53. University of Western Australia, Geology Department and University Extension Publication **9**.

Clark R. N., Gallagher A. J. & Swayze G. A. 1990. Material absorption-band depth mapping of imaging spectrometer data using the complete band shape least-squares algorithm to simultaneously fit to multiple spectral features from multiple materials. *In: 3rd AVIRIS Workshop, Pasadena, CA*, pp. 176–186. JPL Publication **90-54**.

Clark R. N., King T. V. V. & Gorelick N. 1987. Automatic continuum analysis of reflectance spectra. *Proceedings of the 3rd Airborne Imaging Spectrometer Data Analysis Workshop, Pasadena, CA*, pp. 138–142. JPL Publication **87–30**.

Clark R. N., King T. V. V., Klejwa M. & Swayze G. A. 1990. High spectral resolution reflectance spectroscopy of minerals. *Journal of Geophysical Research* **95B**, 12653–12680.

Clark R. N. & Roush T. L. 1984. Reflectance spectroscopy: quantitative analysis techniques for remote sensing applications. *Journal of Geophysical Research* **89**, 6329–6340.

Clark R. N., Swayze G. A., Wise R., Livo K. E., Hoefen T. M., Kokaly R. F. & Sutley S. J. 2003. *USGS Digital Spectral Library splib05a*. US Geological Survey Open File Report **03–395**.

Cockell C. S. & Barlow N. G. 2002. Impact excavation and the search for subsurface life on Mars. *Icarus* **155**, 340–349.

Cocks T., Jenssen R., Stewart A., Wilson I. & Shields T. 1998. The HyMap airborne hyperspectral sensor: the system, calibration and performance. *In: 1st EARSeL Conference*, pp. 37–42.

Cudahy T. J. 2004. Mapping alteration zonation associated with volcanic massive sulphide mineralisation using airborne hyperspectral data. In: McConachy T. F. & McInnes B. A. I. eds. *CSIRO Explores: Copper–Zinc Massive Sulphide Deposits in Western Australia*, vol. 2 pp. 117–124. CSIRO, Perth.

Deer W. A., Howie R. A. & Zussman J. 1992. *An Introduction to the Rock Forming Minerals*. Longman, Harlow.

Dunlop J. S. R. & Buick R. 1981. Archaean epiclastic sediments derived from mafic volcanics, North Pole, Pilbara Block, Western Australia. *In:* Groves D. I. & Glover J. E. eds. *Archaean Geology. Proceedings 2nd International Sympsoium, Perth 1980*, pp. 225–233. Geological Society of Australia Special Publication **7**.

Dunlop J. S. R., Muir M. D., Milne V. A. & Groves D. I. 1978. A new microfossil assemblage from the Archaean of Western Australia. *Nature* **274**, 676–678.

Farmer J. D. 1996. Hydrothermal systems on Mars: an assessment of present evidence. *In:* Bock G. R. & Goode J. A. eds. *Evolution of Hydrothermal Ecosystems on Earth (and Mars?)*, pp. 273–299. CIBA Foundation Symposia Series **202**.

Farr T. G. 2004. Terrestrial analogs to Mars: the NRC community decadal report. *Planetary and Space Science* **52**, 3–10.

Gao B-C., Heidebrecht K. B. & Goetz A. F. H. 1993. Derivation of scaled surface reflectances from AVIRIS data. *Remote Sensing of Environment* **44**, 165–178.

Goetz A. F. H., Rock B. N. & Rowan L. C. 1983. Remote sensing for exploration. *Economic Geology* **78**, 573–590.

Groves D. I., Dunlop J. S. R. & Buick R. 1981. An early habitat of life. *Scientific American* **245**, 56–65.

Gulick V. C. 1998. Magmatic intrusions and a hydrothermal origin for fluvial valleys on Mars. *Journal of Geophysical Research* **103E**, 19365–19387.

Harrison K. P. & Grimm R. E. 2002. Controls on Martian hydrothermal systems: application to valley network and magnetic anomaly formation. *Journal of Geophysical Research* **107E**, Article 5025.

Hellman M. J. & Ramsey M. S. 2004. Analysis of hot springs and associated deposits in Yellowstone National Park using ASTER and AVIRIS remote sensing. *Journal of Volcanology and Geothermal Research* **135**, 195–219.

Hofmann H. J., Grey K., Hickman A. H. & Thorpe R. I. 1999. Origin of 3.45 Ga coniform stromatolites in Warrawoona Group, Western Australia. *Geological Society of America Bulletin* **111**, 1256–1262.

Hunt G. R. 1979. Near infrared (1.3–2.4 μm) spectra of alteration minerals—potential for use in remote sensing. *Geophysics* **44**, 1974–1986.

Kashefi K. & Lovley D. R. 2003. Extending the upper temperature limit for life. *Science* **301**, 934.

Kirkland L. E., Herr K. C. & Adams P. M. 2003. Infrared stealthy surfaces: why TES and THEMIS may miss some substantial mineral deposits on Mars and implications for remote sensing of planetary surfaces. *Journal of Geophysical Research* **2003E**, Article 5137.

Kirkland L., Herr K., Keim E., Adams P., Salisbury J., Hackwell J. & Treiman A. 2002. First use of an airborne thermal infrared hyperspectral scanner for compositional mapping. *Remote Sensing of Environment* **80**, 447–459.

Kirkland L. E., Herr K. C. & Salisbury J. W. 2001. Thermal infrared spectral band detection limits for unidentified surface materials. *Applied Optics* **40**, 4852–4862.

Kitajima K., Maruyama S., Utsunomiya S. & Liou J. G. 2001. Seafloor hydrothermal alteration at an Archaean mid-ocean ridge. *Journal of Metamorphic Geology* **19**, 581–597.

Kokaly R. F., Clark R. N. & Livo K. E. 1998. Mapping the biology and mineralogy of Yellowstone National Park using imaging spectroscopy. *In: 7th AVIRIS Conference, Pasadena, CA*, pp. 245–250. JPL Publication **97-21**.

Lowe D. R. 1980. Stromatolites 3,400-Myr old from the Archaean of Western Australia. *Nature* **284**, 441–443.

Lowe D. R. 1983. Restricted shallow-water sedimentation of early Archean stromatolitic and evaporitic strata of the Strelley Pool Chert, Pilbara Block, Western Australia. *Precambrian Research* **19**, 239–283.

Lowell J. D. & Guilbert J. M. 1970. Lateral and vertical alteration–mineralization zoning in porphyry ore Deposits. *Economic Geology* **65**, 373–408.

McCord T. B. 1988. Reflectance spectroscopy in planetary science: reviews and strategy for the future. *NASA Special Publication* **SP-493**.

Meyer C. & Hemley J. J. 1967. Wallrock alteration. *In:* Barnes H. L. ed. *Geochemistry of Hydrothermal Ore Deposits*, pp. 166–235. Holt, Rinehart & Wilson, New York.

Mustard J. F. & Hays J. E. 1997. Effects of hyperfine particles on reflectance spectra from 0.3 to 25 mu m. *Icarus* **125**, 145–163.

NASA 1995. An exobiological strategy for Mars exploration. *NASA Special Publication* **SP-530**.

Nealson K. H. 1997. The limits of life on Earth and searching for life on Mars. *Journal of Geophysical Research Planets* **102E**, 23675–23686.

Nisbet E. G. & Sleep N. H. 2001. The habitat and nature of early life. *Nature* **409**, 1083–1091.

Pontual S. 1997. *G-Mex Volume 1: Special Interpretation Field Manual*. Ausspec International, Kew.

Rowan L. C., Simpson C. J. & Mars J. C. 2004. Hyperspectral analysis of the ultramafic complex and adjacent lithologies at Mordor, NT, Australia. *Remote Sensing of Environment* **91**, 419–431.

Schopf J. W. 1993. Microfossils of the Early Archaean Apex Chert: new evidence of the antiquity of life. *Science* **260**, 640–646.

Schott J. R. 1996. *Remote Sensing: The Image Chain Approach*, Oxford University Press, New York.

Shock E. L. 1997. High-temperature life without photosynthesis as a model for Mars. *Journal of Geophysical Research* **102E**, 23687–23694.

Sillitoe R. H. 1993. Epithermal models: genetic types, geometrical controls and shallow features. *Geological Association of Canada Special Paper* **40**, 403–417.

Singer R. B. & Roush T. L. 1985. Effects of temperature on remotely sensed mineral absorption features. *Journal of Geophysical Research* **90**, 12434–12444.

Space Studies Board 2003. *New Frontiers in the Solar System: An Integrated Exploration Strategy*. National Research Council, Washington.

Stamoulis V., Mauger A. J. & Cudahy T. J. 2001. Mapping mineral abundances of the Musgrave Block, South Australia, using airborne hyperspectral VNIR-SWIR data. *International Geoscience and Remote Sensing Symposium* **7**, 3169.

Terabayashi M., Masada Y. & Ozawa H. 2003. Archean ocean-floor metamorphism in the North Pole area, Pilbara Craton, Western Australia. *Precambrian Research* **127**, 167–180.

Thomas M. & Walter M. R. 2002. Application of hyperspectral infrared analysis of hydrothermal alteration on Earth and Mars. *Astrobiology* **2**, 335–351.

Thompson A. J. B. & Thompson J. F. H. 1996. *Atlas of Alteration: a Field and Petrographic Guide to Hydrothermal Alteration Minerals*. Geological Association of Canada, Mineral Deposits Division, St. John's.

Thorpe R. I., Hickman A. H., Davis D. W., Mortensen J. K. & Trendall A. F. 1992. U–Pb zircon geochronology of Archaean felsic units in the Marble Bar region, Pilbara Craton, Western Australia. *Precambrian Research* **56**, 169–189.

Ueno Y., Yoshioka H., Maruyama S. & Isozaki Y. 2004. Carbon isotopes and petrography of kerogens in ~3.5-Ga hydrothermal silica dikes in the North Pole area, Western Australia. *Geochimica et Cosmochimica Acta* **68**, 573–589.

Vago J. L., Gardini B. & Kminek G. 2003. ESA's new mission to search for signs of life on Mars: ExoMars and its Pasteur scientific payload. *EGS–AGU–EUG Joint Assembly, Nice, France*, p. 2504.

Van Kranendonk M. J. 2000. *Geology of the North Shaw 1:100 000 Sheet*. Geological Survey of Western Australia, Perth.

Van Kranendonk M. & Hickman A. H. 2000. Archaean geology of the North Shaw region, East Pilbara Granite Greenstone Terrain, Western Australia—a field guide. *Geological Survey of Western Australia Record* **2000/5**.

Van Kranendonk M. J. & Pirajno F. 2004. Geochemistry of metabasalts and hydrothermal alteration zones associated with ca. 3.45 Ga chert+/– barite deposits: implications for the geological setting of the Warrawoona Group, Pilbara Craton, Australia. *Geochemistry: Exploration, Environment and Analysis* **4**, 253–278.

Varnes E. S., Jakosky B. M. & McCollom T. M. 2003. Biological potential of Martian hydrothermal Systems. *Astrobiology* **3**, 407–414.

Vincent R. K. & Hunt G. R. 1968. Infrared reflectance from mat surfaces. *Applied Optics* **7**, 53–58.

Walter M. R., Buick R. & Dunlop J. S. R. 1980. Stromatolites 3400–3500 Myr old from the North Pole area, Western Australia. *Nature* **284**, 443–445.

Walter M. R. & Des Marais D. J. 1993. Preservation of biological information in thermal-spring deposits – developing a strategy for the search for fossil life on Mars. *Icarus* **101**, 129–143.

Wendlandt W. W. & Hecht H. G. 1966. *Reflectance Spectroscopy*. Wiley-Interscience, New York.

Received 30 June 2004; accepted 4 March 2005